

STUDY OF HEAT TRANSFER EFFECTS ON UNSTEADY FREE CONVECTIVE MHD FLOW

In this Chapter, Heat transfer effects on unsteady free convective MHD flow of incompressible micro-polar fluid and motion takes place due to the buoyancy force between two vertical walls have been considered. Momentum, angular momentum and energy equations are converted to the system of linear partial differential equations with initial boundary conditions using dimensionless variable. To check the accuracy of the numerical solution obtained by Matlab software, a comparison of the steady-state numerical solution with the analytical solution of the corresponding steady flow with tabular form. For better understanding of physical aspects, considering effects of various physical parameters on velocity, micro-rotation and temperature profiles as shown graphically (Refer Figures 2.2 to 2.18).

2.1 Introduction of the problem

Recently, the study of micro-polar fluid has been concerned several researchers as Navier–Stokes equations of Newtonian fluids cannot describe the features of fluid with suspended particles effectively. Eringen [2] presented the concept of micro-polar fluid, this idea is useful in clarifying the characteristics of certain fluids such as liquid crystals, suspensions and animal blood. Chamkha et al. [17] and Alloui et al. [21] studied applications of micro-polar fluids in vertical channel.

Research works on MHD have been significantly advanced during the last few years in natural sciences and engineering disciplines after the pioneer work of Hartmann [8] in liquid metal duct flows under the influence of a strong external magnetic field. Haque et al. [79] considered micro-polar fluid behaviors on steady MHD free convection flow. Heat transfer can be obtained as the transmission of energy from one region to another as a result of temperature difference between them. The study of flow and heat transfer of an electrically conduct micro-polar fluid under the influence of a magnetic field, a large number of researchers have worked on the subjects and its applications are enormous of many engineering, nuclear reactors and biological science. In contrast, further study has been carried out by Sudhakara et al. [24] heat transfers in a thin film flow of a micro-polar fluids and Eldabe and Salwa [45] examined heat transfer effects on MHD Casson fluid flow between two rotating cylinders. Recently, Abbas et al. [65] considered heat transfer effects on MHD flow on a stretching sheet in a rotating fluid. The study of MHD flow of micro-polar fluid

between two vertical walls is an important in fluid mechanics and its huge application in science and technology. Prakash and Muthamilselvan [93] discussed radiation effects on transient MHD flow of micro-polar fluid.

2.2 Novelty of the Problem

In the most of the previous research works, case of asymmetric or symmetric thermal condition are studied in absence of magnetic field. In this chapter, a detailed analysis of how an unsteady free convective flow of micro-polar fluid behave in symmetric/asymmetric wall temperature by influence of magnetic field. The Numerical solution of this problems have been worked out using Matlab software. The validation of results, like velocity, micro-rotation and temperature profiles are derived from analytically for steady state case and also compared with numerical results as obtained with the Matlab software.

2.3 Mathematical formulation of the Problem

Consider the unsteady free-convective flow of an electric conductive micro-polar fluid between two insulated vertical walls separated by a distance L apart subjected to a uniform transverse magnetic field. The coordinate system is chosen such that x' measures the distance along the walls and y' measures the distance normal to it. Initially, the temperatures of walls and the fluid are same, presents T_f' . If time $t' > 0$, the temperature of the walls at $y' = 0$ and $y' = L$ is instantaneously raised and lowered to T_h' and T_c' respectively such that $T_h' > T_c'$ later the temperature remains constant. Also, a constant uniformly distributed transverse magnetic field of strength B_0 is applied in the y' -direction which is shown in Figure 2.1.

Since the transversely applied magnetic field and magnetic Reynolds number are very small so the induced magnetic field is negligible. The Hall effects, the joule heating terms and magnetic dissipations in energy equation are also neglected. The above assumptions and Boussinesq approximation is taken in consideration, the governing partial differential equations of micro-polar fluid can be expressed as follows.

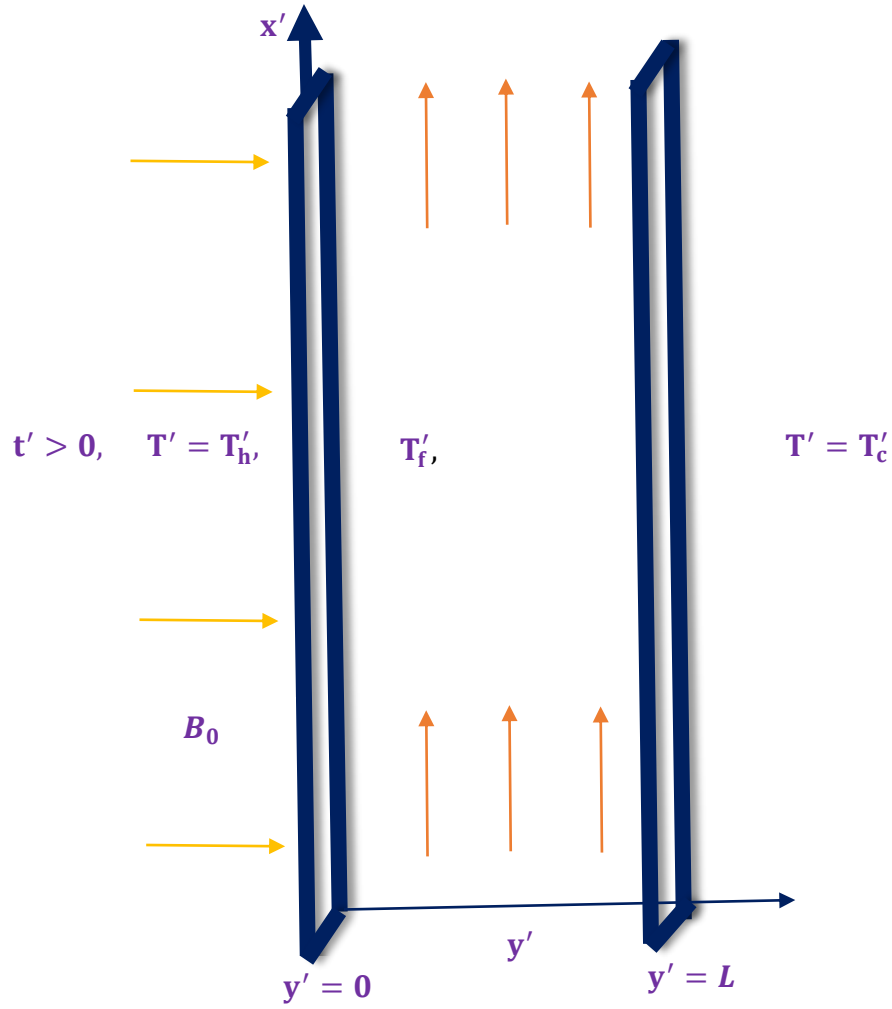


Figure 2.1: Physical Sketch of the Problem

$$\rho \frac{\partial u'}{\partial t'} = (\mu + k_3) \frac{\partial^2 u'}{\partial y'^2} + k_3 \frac{\partial \omega'}{\partial y'} + \rho g \beta'_T (T' - T'_m) - B_0^2 \sigma u' \quad (2.1)$$

$$\rho j \frac{\partial \omega'}{\partial t'} = \left(\mu + \frac{k_3}{2} \right) j \frac{\partial^2 \omega'}{\partial y'^2} - k_3 \left(2\omega' + \frac{\partial u'}{\partial y'} \right) \quad (2.2)$$

$$\frac{\partial T'}{\partial t'} = \frac{k_4}{\rho c_p} \frac{\partial^2 T'}{\partial y'^2} \quad (2.3)$$

Initial & boundary conditions are;

$$\begin{aligned}
 t \leq 0 \quad u' = \omega' = 0, \quad T' = T_f', \quad 0 \leq y' \leq L \\
 t > 0 \quad u' = \omega' = 0, \quad T' = T_h', \quad y' = 0 \\
 u' = \omega' = 0, \quad T' = T_c', \quad y' = L
 \end{aligned} \tag{2.4}$$

Introducing the following similarity transformations in Equations (2.1) - (2.4);

$$\begin{aligned}
 y = \frac{y'}{L}, t = \frac{v t'}{L^2}, u = \frac{u' v}{\beta_T' g L^2 (T_h' - T_m')}, \theta = \frac{(T' - T_m')}{(T_h' - T_m')}, \omega = \frac{\omega' v}{\beta_T' g L (T_h' - T_m')}, Pr = \frac{\rho C_p}{k_4}, \\
 m_1 = \frac{(T_c' - T_m')}{(T_h' - T_m')}, b = \frac{L^2}{j}, R = \frac{k_3}{\mu}, M = \frac{B_0^2 \sigma L^2}{\mu}
 \end{aligned} \tag{2.5}$$

The following linear system of differential equations and corresponding initial boundary conditions can be framed as follows;

$$\frac{\partial u}{\partial t} = (1 + R) \frac{\partial^2 u}{\partial y^2} + \theta + R \frac{\partial \omega}{\partial y} - M^2 u \tag{2.6}$$

$$\frac{\partial \omega}{\partial t} = (1 + 0.5 R) \frac{\partial^2 \omega}{\partial y^2} - R b \left(\frac{\partial u}{\partial y} + 2\omega \right) \tag{2.7}$$

$$\frac{\partial \theta}{\partial y} = \frac{1}{Pr} \frac{\partial^2 \theta}{\partial y^2} \tag{2.8}$$

$$\begin{aligned}
 t \leq 0 \quad u = \omega = \theta = 0 \quad 0 \leq y \leq 1; \\
 t > 0 \quad u = \omega = 0, \quad \theta = 1; \quad y = 0 \\
 u = \omega = 0, \quad \theta = m_1; \quad y = 1
 \end{aligned} \tag{2.9}$$

2.4 Numerical solution

The governing linear system partial differential equations (2.6) to (2.8) with initial boundary conditions are solved numerically using Matlab software. The increment step of time variable t with 0.05 and direction y with 0.0323 are divided in entire numerical computations. In present problem, the accuracy of the solution depend strongly on length of the vector y . By dividing as space y spatial interval $[0,1]$ in 31 parts and the values of time interval $[0,2]$ in 40 parts, finally a mesh has been produced which depicted solution of the problem.

2.5 Steady state Analytical solution

As it is steady state condition, left hand side of Equations (2.6), (2.7) and (2.8) become zero hence, there is only one independent variable which becomes the case of ordinary differential equations.

From Appendix the steady state analytic result as follows;

Case-I $a_1 \neq 0, a_2 \neq 0$

$k > 0$, $k = p^2$

(i) $p_1 > 0$ & $p_2 > 0$

$$w = c_1 e^{\sqrt{p_1}y} + c_2 e^{-\sqrt{p_1}y} + c_3 e^{-\sqrt{p_2}y} + c_4 e^{-\sqrt{p_2}y} + A \quad (2.10)$$

$$u = b_{10} e^{p_1 y} - b_{11} e^{-p_1 y} + c_3 b_6 e^{p_2 y} - c_4 b_6 e^{-p_2 y} + A_6 y + A_7 \quad (2.11)$$

(ii) $p_1 > 0$ & $p_2 < 0$

$$w = c_5 e^{\sqrt{p_1}y} + c_6 e^{-\sqrt{p_1}y} + c_7 \cos\sqrt{p_2}y + c_8 \sin\sqrt{p_2}y + A \quad (2.12)$$

$$u = b_{15} e^{p_1 y} - b_{16} e^{-p_1 y} + c_7 b_{12} \sin p_2 y - c_8 b_{12} \cos p_2 y + A_6 y + A_7 \quad (2.13)$$

(iii) $p_1 < 0$ & $p_2 > 0$

$$w = c_9 \cos\sqrt{p_1}y + c_{10} \sin\sqrt{p_1}y + c_{11} e^{-\sqrt{p_2}y} + c_{12} e^{-\sqrt{p_2}y} + A \quad (2.14)$$

$$u = b_{18} \sin p_1 y + b_{19} \cos p_1 y + c_{11} b_6 e^{p_2 y} - c_{12} b_6 e^{-p_2 y} + A_6 y + A_7 \quad (2.15)$$

(iv) $p_1 < 0$ & $p_2 < 0$

$$w = c_{13} \cos\sqrt{p_1}y + c_{14} \sin\sqrt{p_1}y + c_{15} \cos\sqrt{p_2}y + c_{16} \sin\sqrt{p_2}y + A \quad (2.16)$$

$$u = b_{20} \sin p_1 y + b_{21} \cos p_1 y + c_{15} b_{12} \sin p_2 y e^{p_2 y} - c_{16} b_{12} \cos p_2 y + A_6 y + A_7 \quad (2.17)$$

$k = 0$

(i) $a_1 > 0$

$$w = (c_{17} + c_{18}y) e^{\sqrt{\frac{a_1}{2}}y} + (c_{19} + c_{20}y) e^{-\sqrt{\frac{a_1}{2}}y} + A \quad (2.18)$$

$$u = (b_{29} + b_{30}y) e^{q_1 y} + (b''_{29} + b''_{30}y) e^{-q_1 y} + A_6 y + A_7 \quad (2.19)$$

(ii) $a_1 < 0$

$$w = (c_{21} + c_{22}y)\cos\sqrt{\frac{a_1}{2}}y + (c_{23} + c_{24}y)\sin\sqrt{\frac{a_1}{2}}y + \frac{a_3}{a_2} \quad (2.20)$$

$$u = (b_{34} + b_{35}y)\sin q_1y + (b_{36} + b_{37}y)\cos q_1y + A_6y + A_7 \quad (2.21)$$

$$k < 0, k = -p^2$$

$$w = e^{v_2y}((c_{25} + c_{26}y)\cos v_1y + (c_{27} + c_{28}y)\sin v_1y) + \frac{a_3}{a_2} \quad (2.22)$$

$$u = (b_{72} + b_{73}y)e^{v_2y}\cos v_1y + (b_{36} + b_{37}y)e^{v_2y}\sin v_1y + A_6y + A_7 \quad (2.23)$$

Case-II $a_1 = 0, a_2 \neq 0$

$$w = e^{\sqrt{\frac{a_2}{2}}y} \left((c_{29} + c_{30}y)\cos\sqrt{\frac{a_2}{2}}y + (c_{31} + c_{32}y)\sin\sqrt{\frac{a_2}{2}}y \right) + \frac{a_3}{a_2} \quad (2.24)$$

$$u = (b_{82}y + b_{83})e^{q_2y}\cos q_2y + (b_{84}y + b_{85})e^{q_2y}\sin q_2y + A_6y + A_7 \quad (2.25)$$

Case-III $a_1 \neq 0, a_2 = 0$

$$w = c_{33}e^{\sqrt{a_1}y} + c_{34}e^{-\sqrt{a_1}y} + c_{35}\cos\sqrt{a_1}y + c_{36}\sin\sqrt{a_1}y - \frac{y^2 a_3}{2 a_1} \quad (2.26)$$

$$u = (b_{91} - c_{35})e^{ry} + b_{91}e^{-ry} + b_{92}\sin ry + b_{93}\cos ry + b_{94}y + A_7 \quad (2.27)$$

Case-IV $a_1 = 0, a_2 = 0$

$$w = c_{37} + c_{38}y + c_{39}y^2 + c_{40}y^3 + \frac{y^4 a_3}{24} \quad (2.28)$$

$$u = b_{95}y^3 + b_{96}y^2 + b_{97}y + b_{99} \quad (2.29)$$

The steady state solution of equation (2.8) is

$$\theta = 1 + (m_1 - 1)y \quad (2.30)$$

2.6 Result and Discussion

The physical parameters appearing in the model are vortex viscosity parameter R , material parameter b and Prandtl number Pr . Whereas temperature ratio m_1 is having values 0 and 1 for asymmetric and symmetric heating respectively.

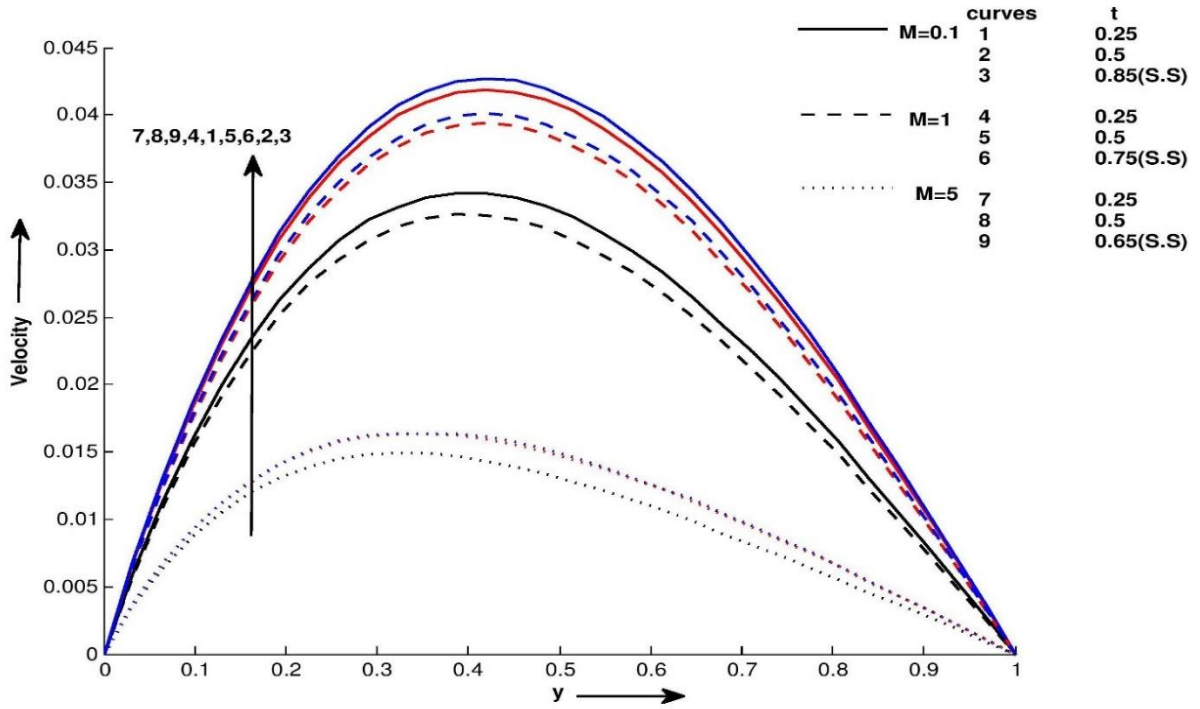


Figure 2.2: Velocity profile u for different values of y at $m_1 = 0, R = 0.5, b = 0.1$ and $Pr = 1$.

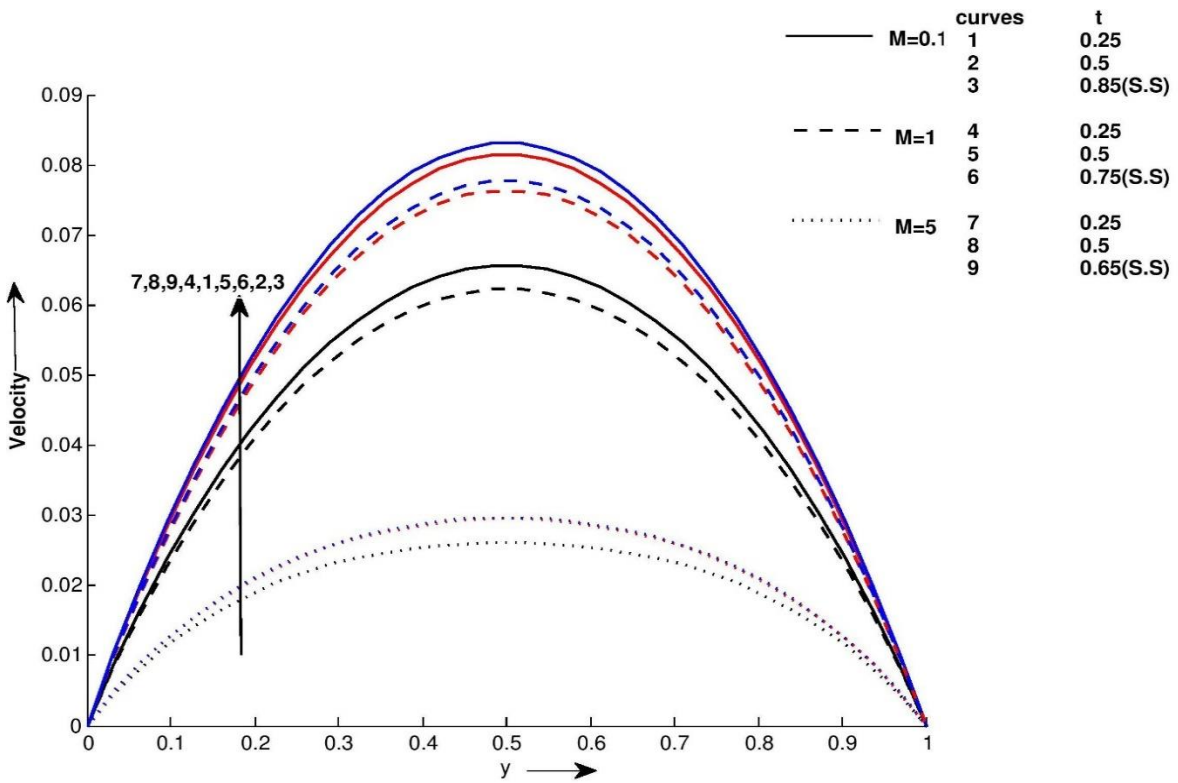


Figure 2.3: Velocity profile u for different values of y at $m_1 = 1, R = 0.5, b = 0.1$ and $Pr = 1$.

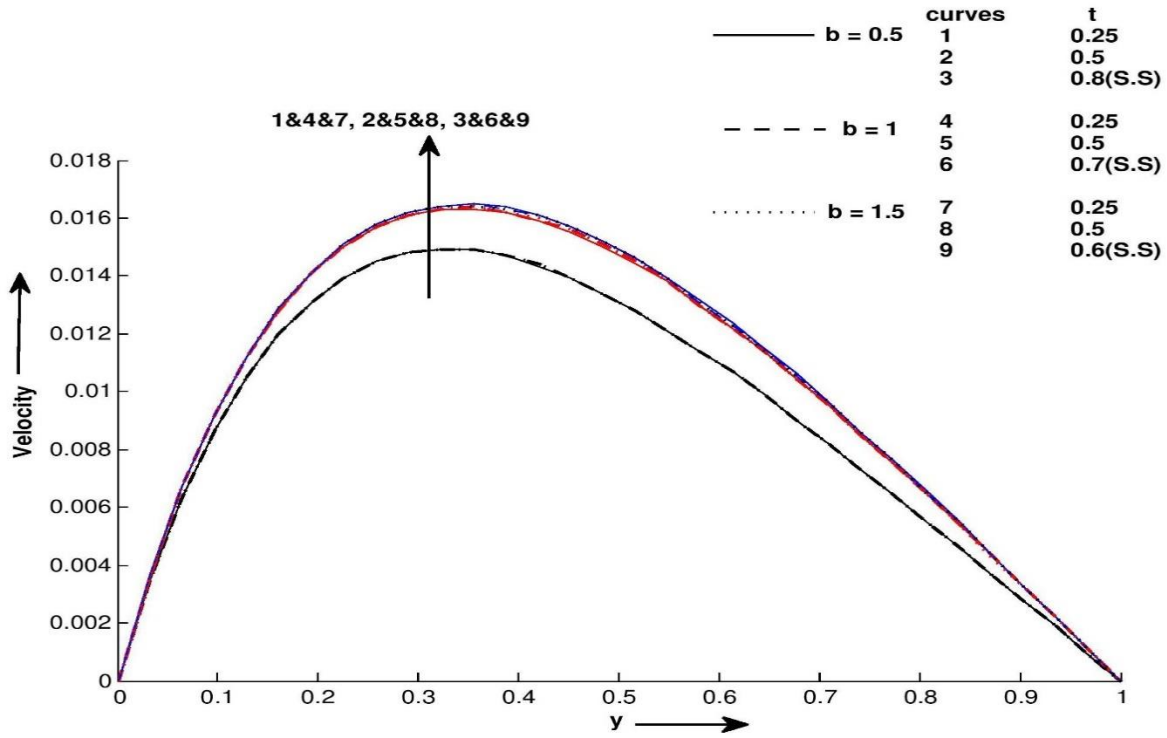


Figure 2.4: Velocity profile u for different values of y at $m_1 = 0, R = 0.5, M = 5$ and $Pr = 1$.

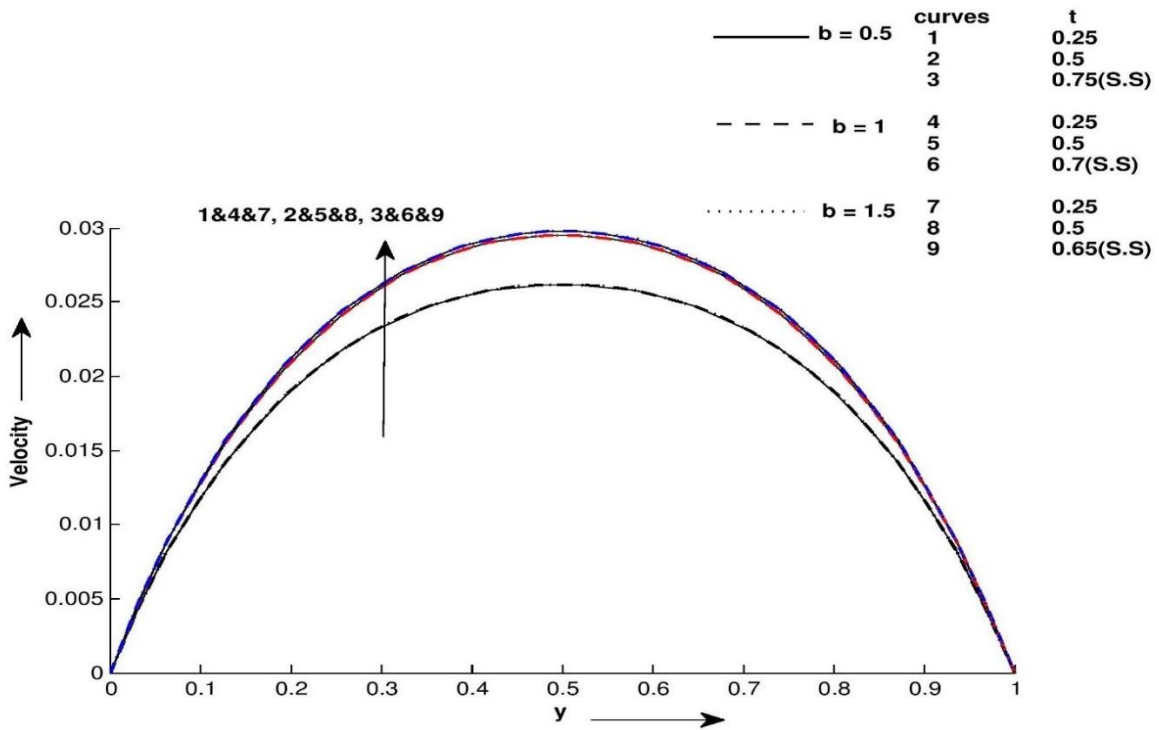


Figure 2.5: Velocity profile u for different values of y at $m_1 = 1, R = 0.5, M = 5$ and $Pr = 1$.

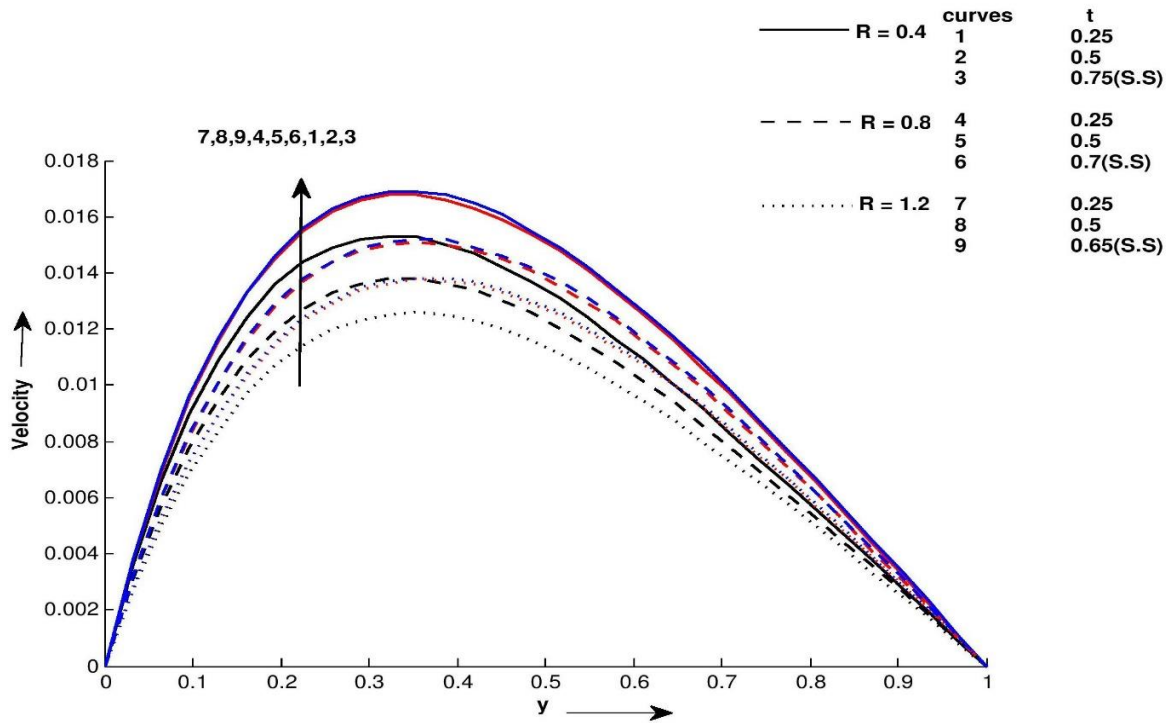


Figure 2.6: Velocity profile u for different values of y at $m_1 = 0, b = 0.1, M = 5$ and $Pr = 1$.

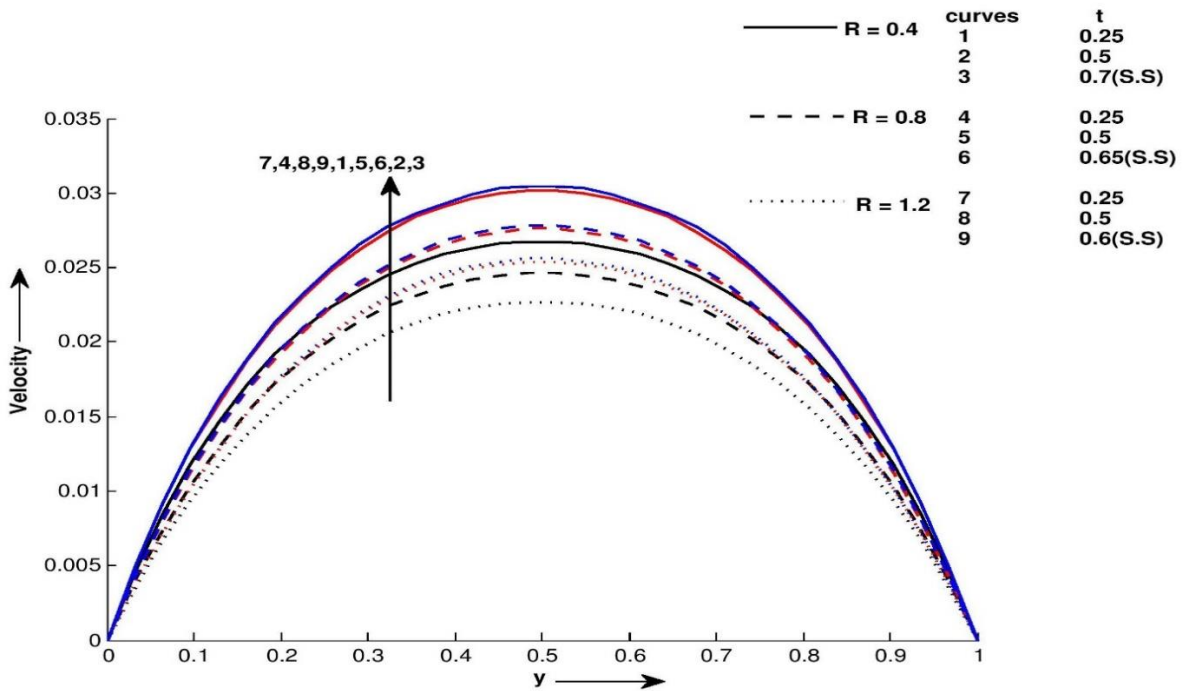


Figure 2.7: Velocity profile u for different values of y at $m_1 = 1, b = 0.1, M = 5$ and $Pr = 1$

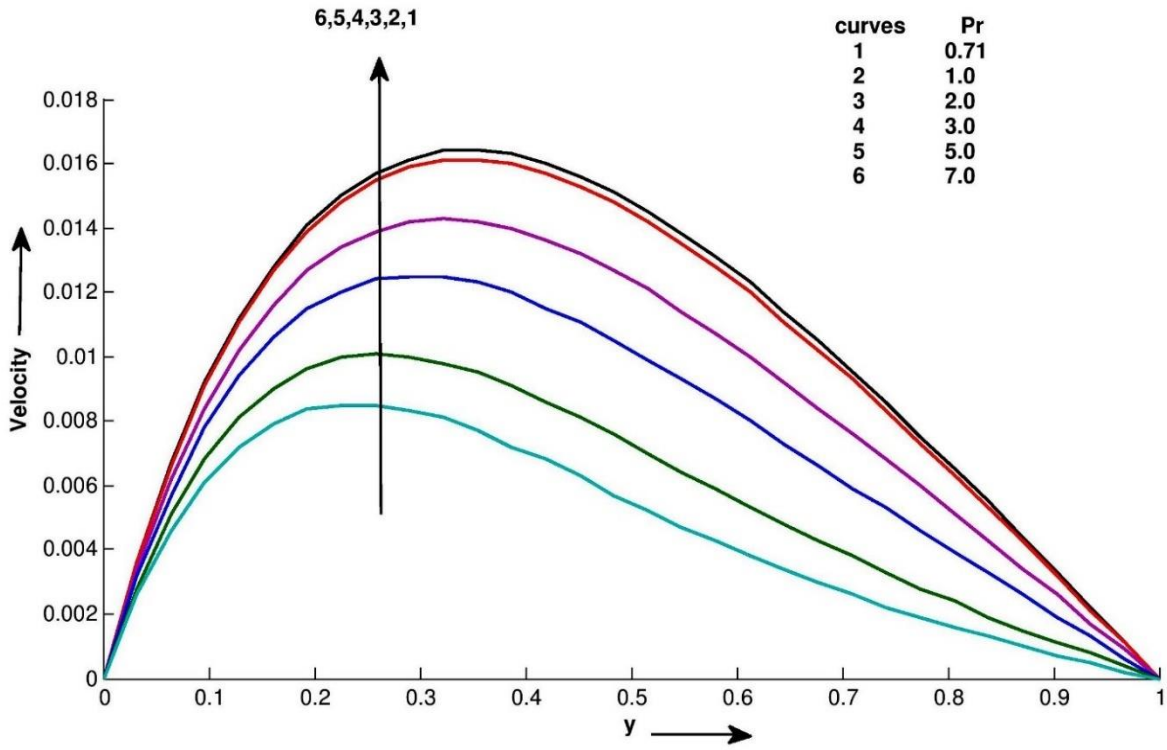


Figure 2.8: Velocity profile u for different values of y at $m_1 = 0, b = 0.1, M = 5$ and $R = 0.5$

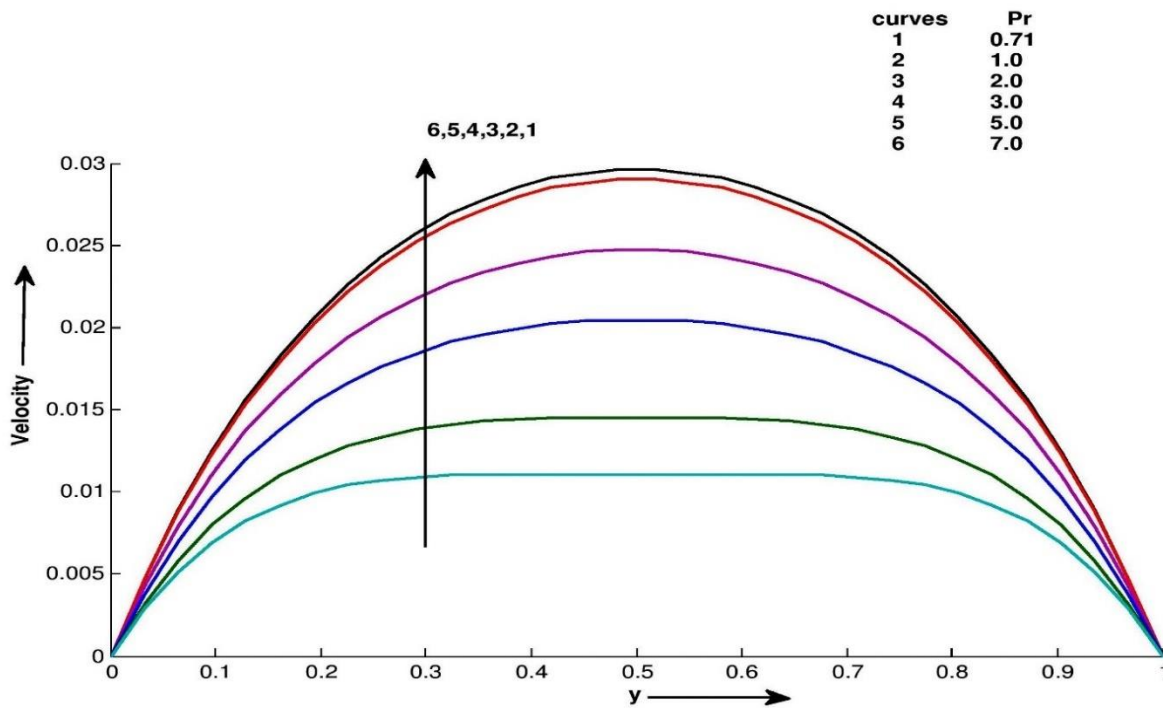


Figure 2.9: Velocity profile u for different values of y at $m_1 = 1, b = 0.1, M = 5$ and $R = 0.5$.

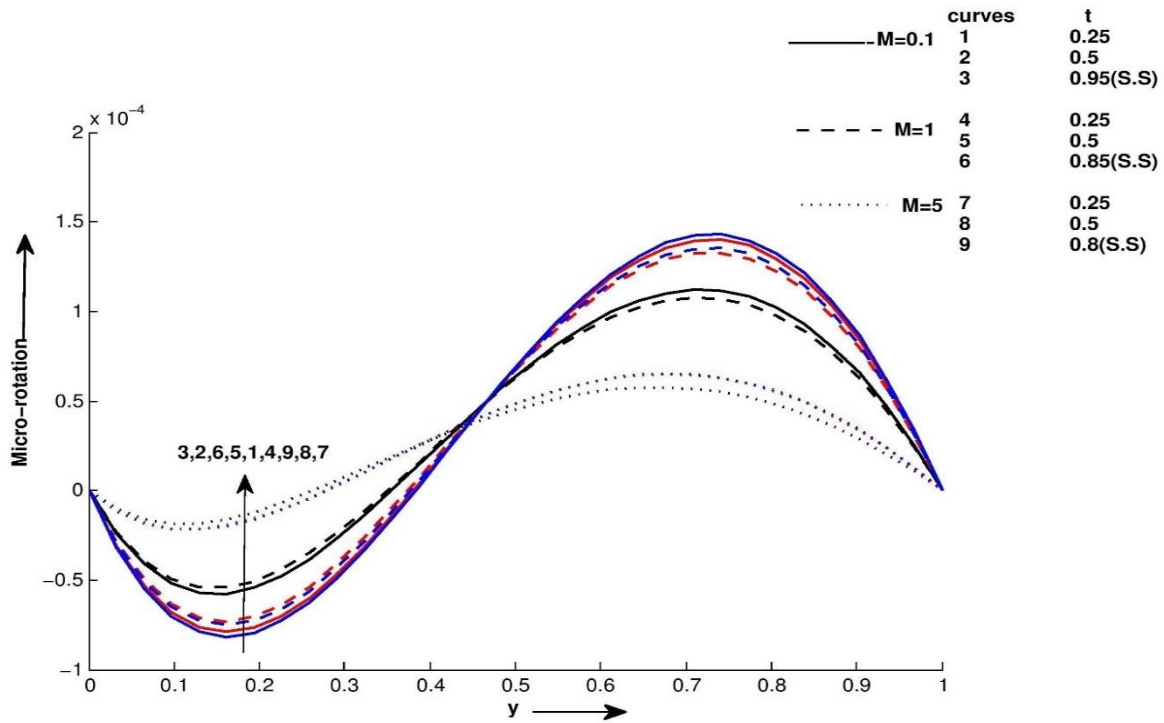


Figure 2.10: Micro-rotation profile ω for different values of y at $m_1 = 0, b = 0.1, Pr = 1$ and $R = 0.5$.

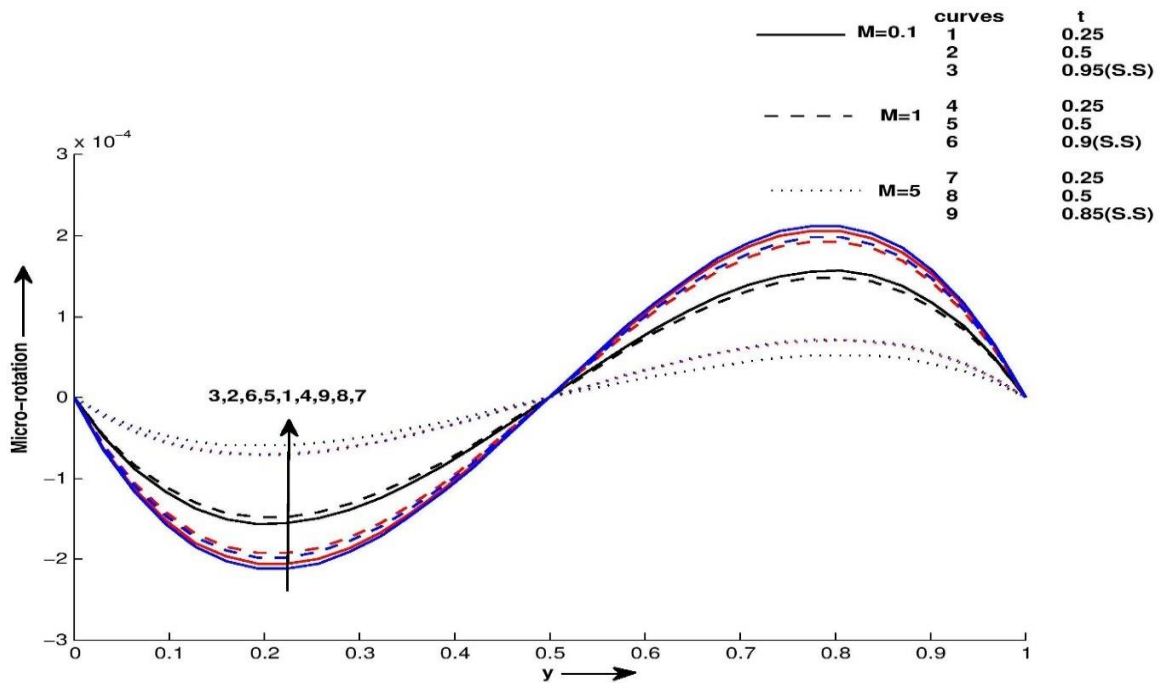


Figure 2.11: Micro-rotation profile ω for different values of y at $m_1 = 1, b = 0.1, Pr = 1$ and $R = 0.5$.

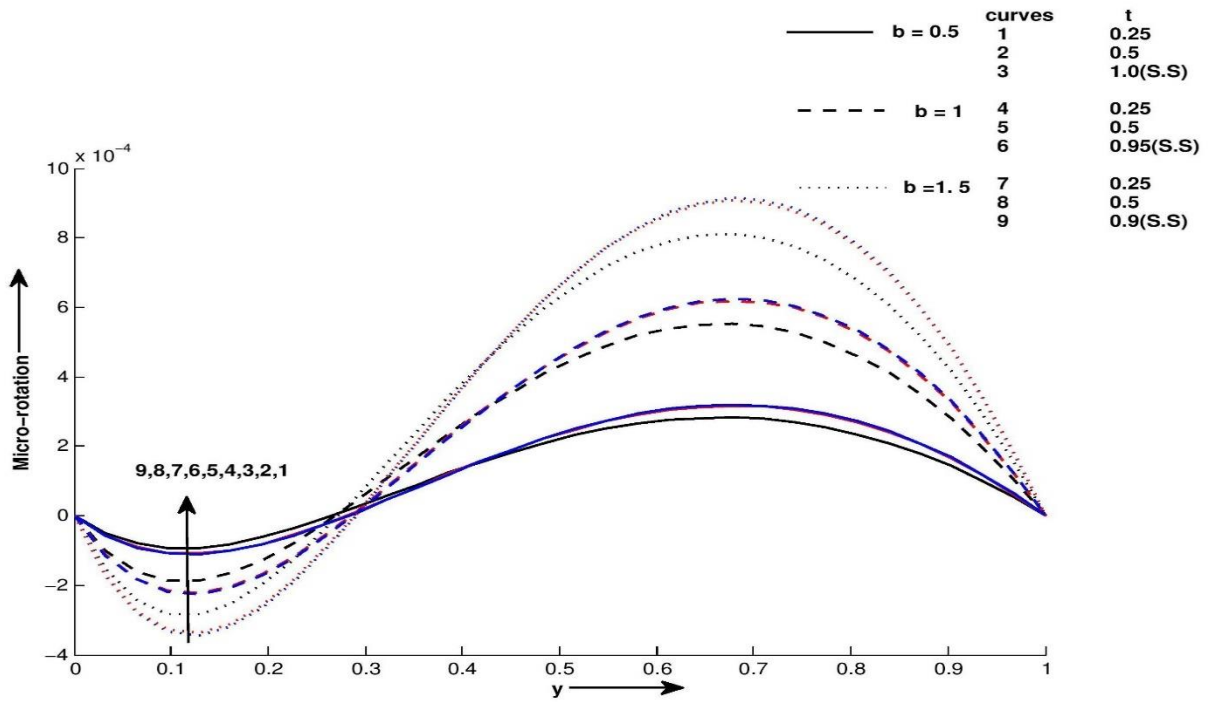


Figure 2.12: Micro-rotation profile ω for different values of y at $m_1 = 0, R = 0.5, M = 5$ and $Pr = 1$.

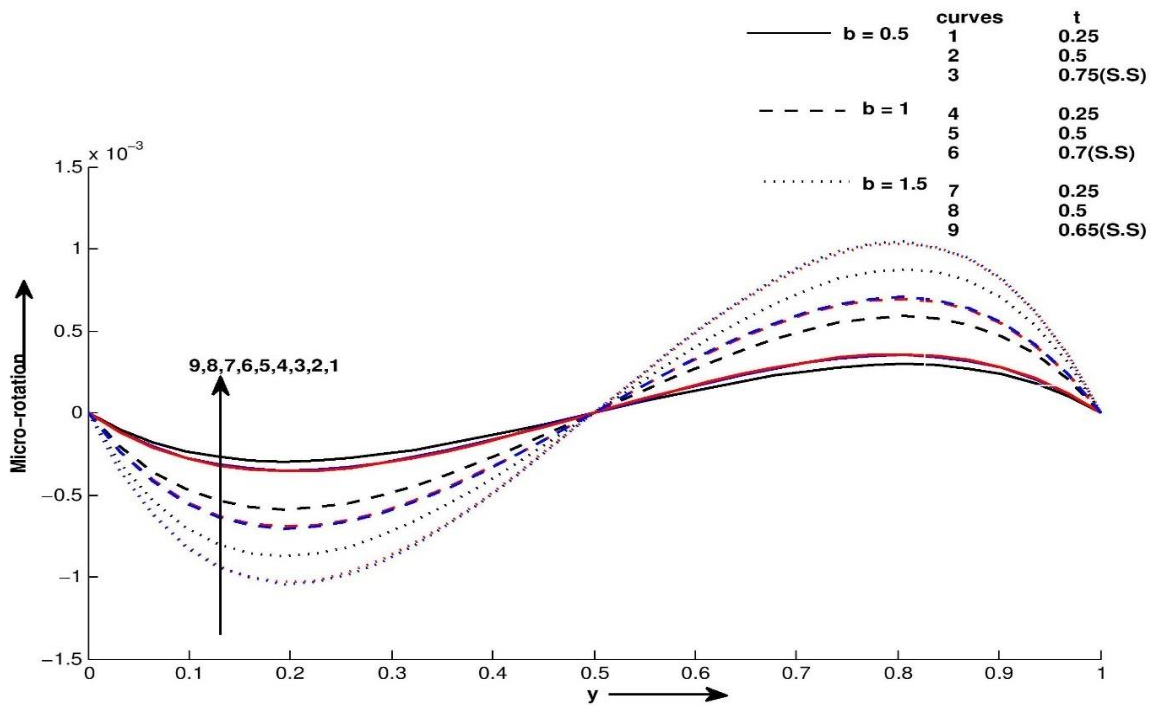


Figure 2.13: Micro-rotation profile ω for different values of y at $m_1 = 1, R = 0.5, M = 5$ and $Pr = 1$

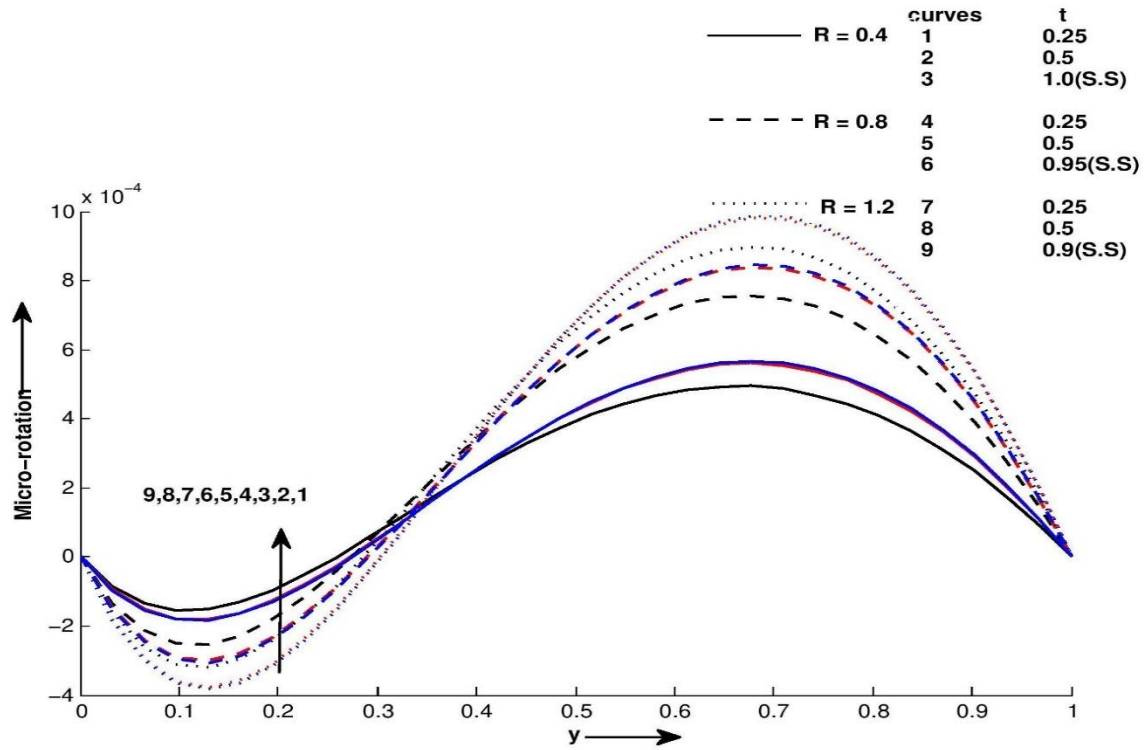


Figure 2.14: Micro-rotation profile w for different values of y at $m_1 = 0, b = 0.1, M = 5$ and $Pr = 1$

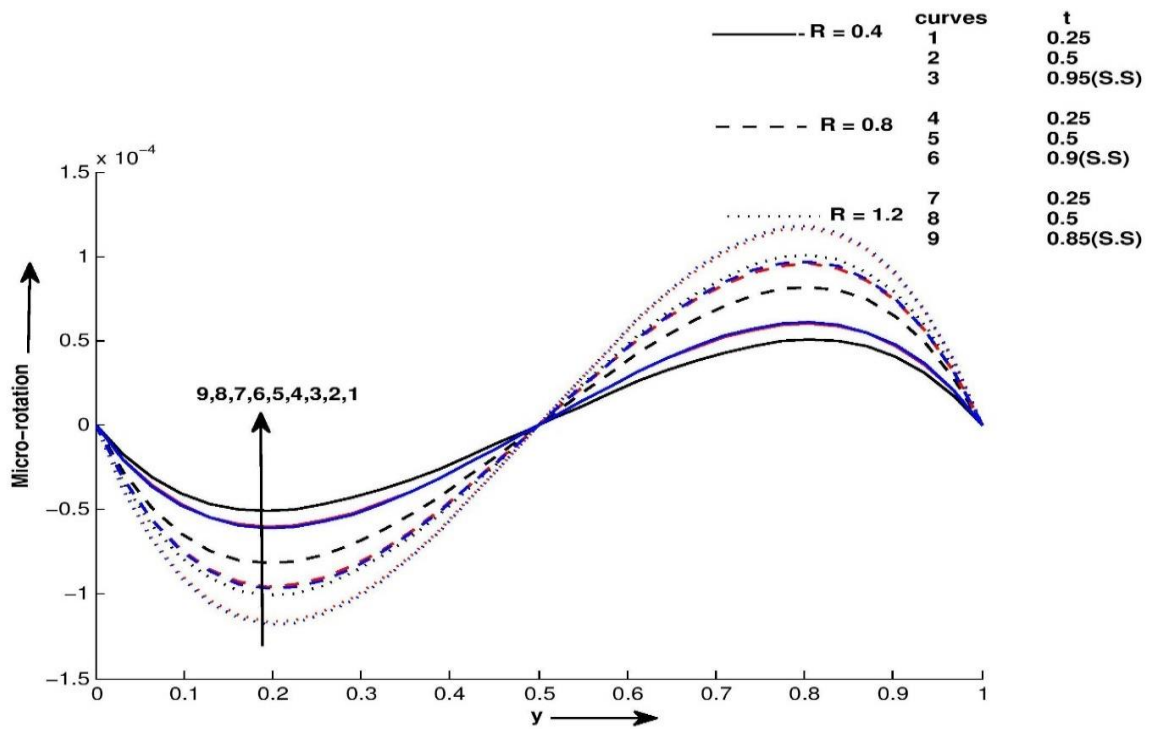


Figure 2.15: Micro-rotation profile ω for different values of y at $m_1 = 1, b = 0.1, M = 5$ and $Pr = 1$.

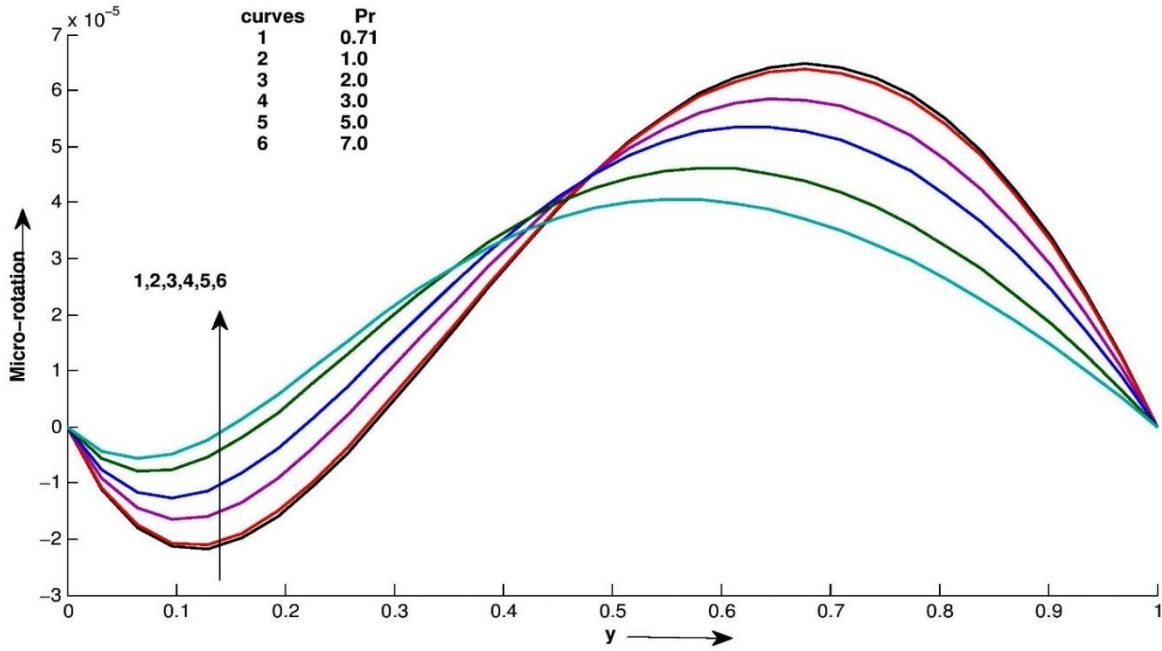


Figure 2.16: Micro-rotation profile ω for different values of y at $m_1 = 0, b = 0.1, M = 5$ and $R = 0.5$.

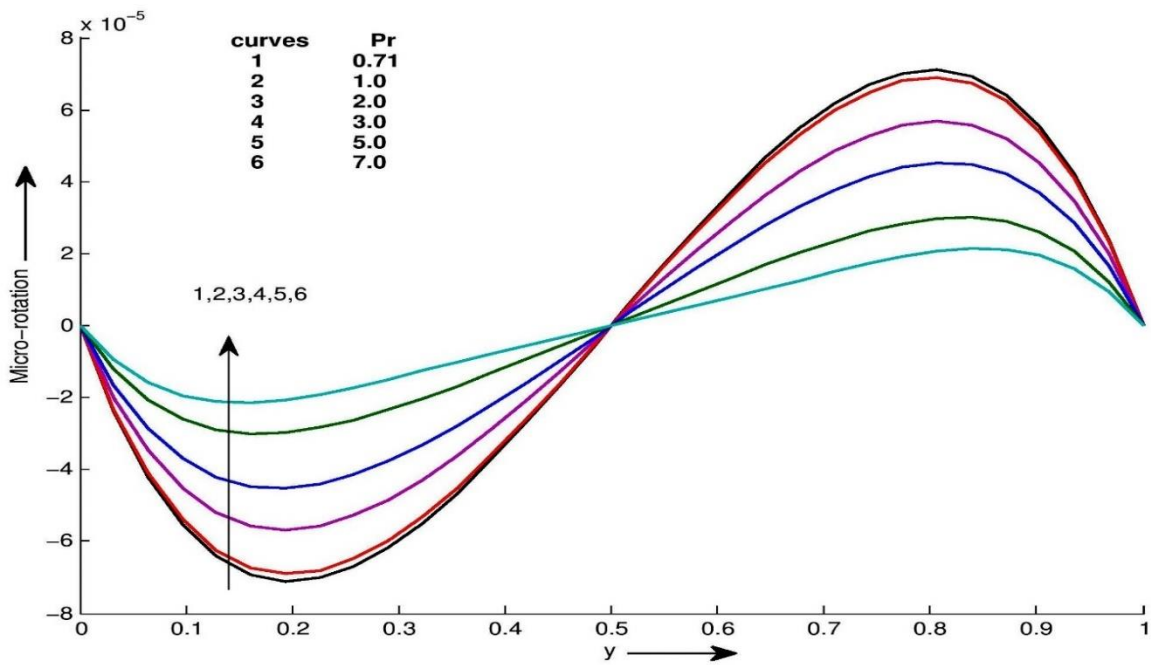


Figure 2.17: Micro-rotation profile ω for different values of y at $m_1 = 1, b = 0.1, M = 5$ and $R = 0.5$

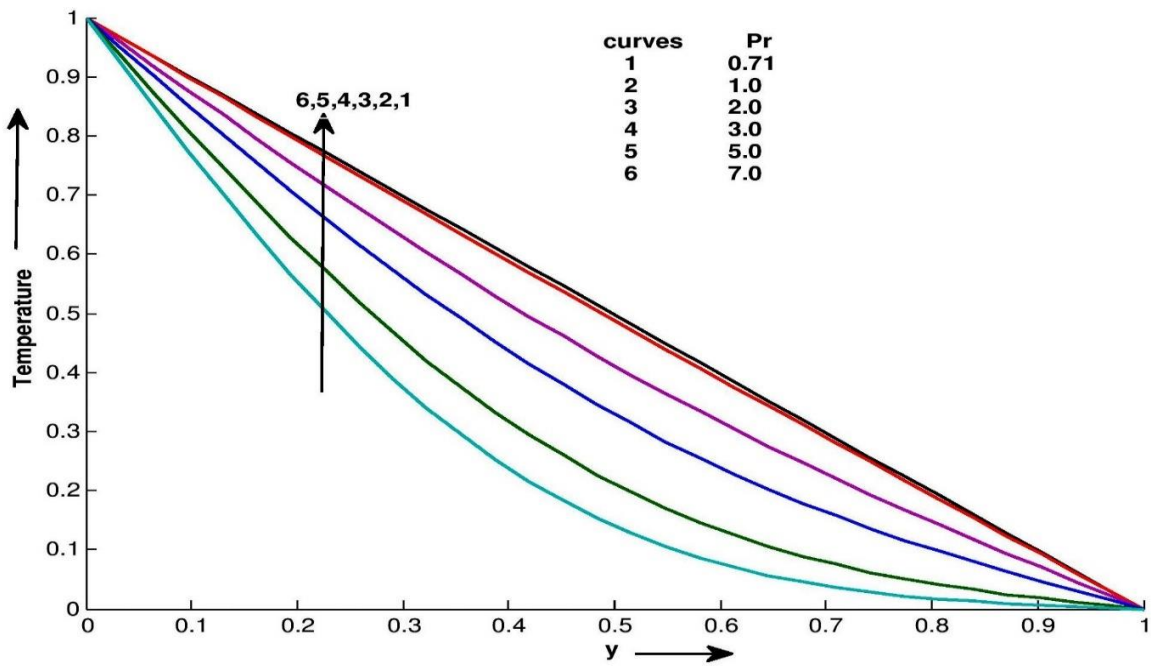


Figure 2.18: Temperature profile θ for different values of y at $m_1 = 0$.

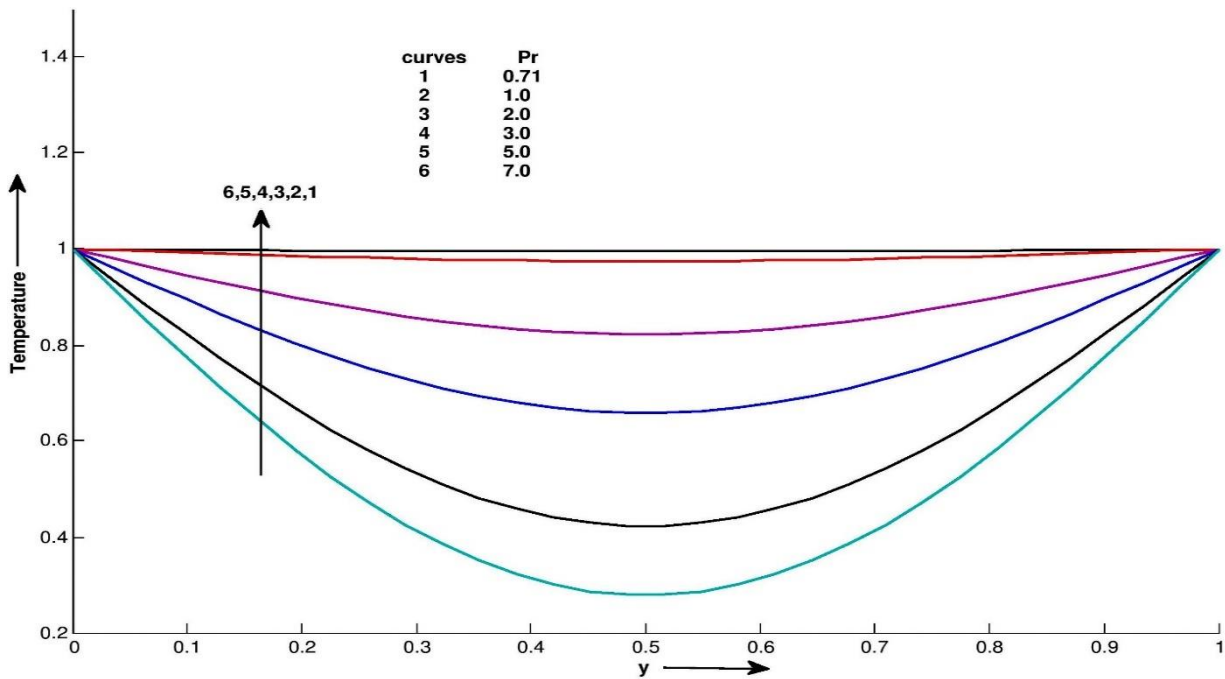


Figure 2.19: Temperature profile θ for different values of y at $m_1 = 1$.

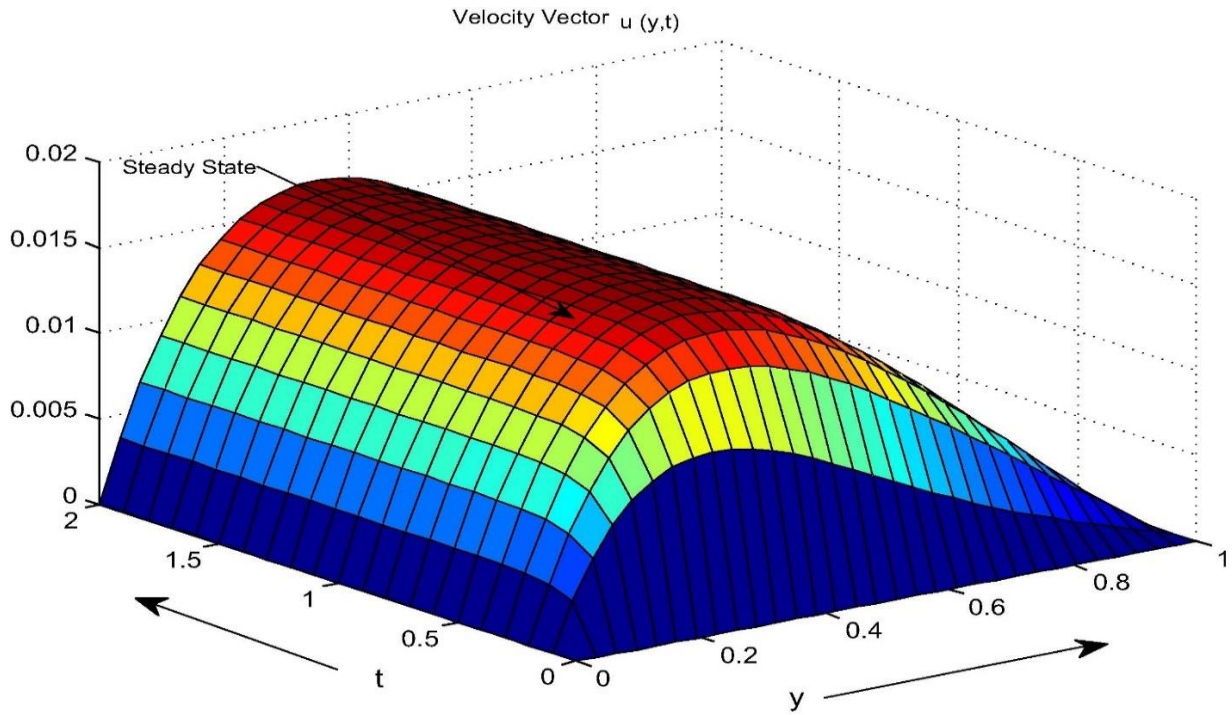


Figure 2.20: Velocity vector $u(y,t)$ for different values of y & t at $m_1 = 0, R = 0.5, b = 0.1, M = 5$ and $Pr = 1$.

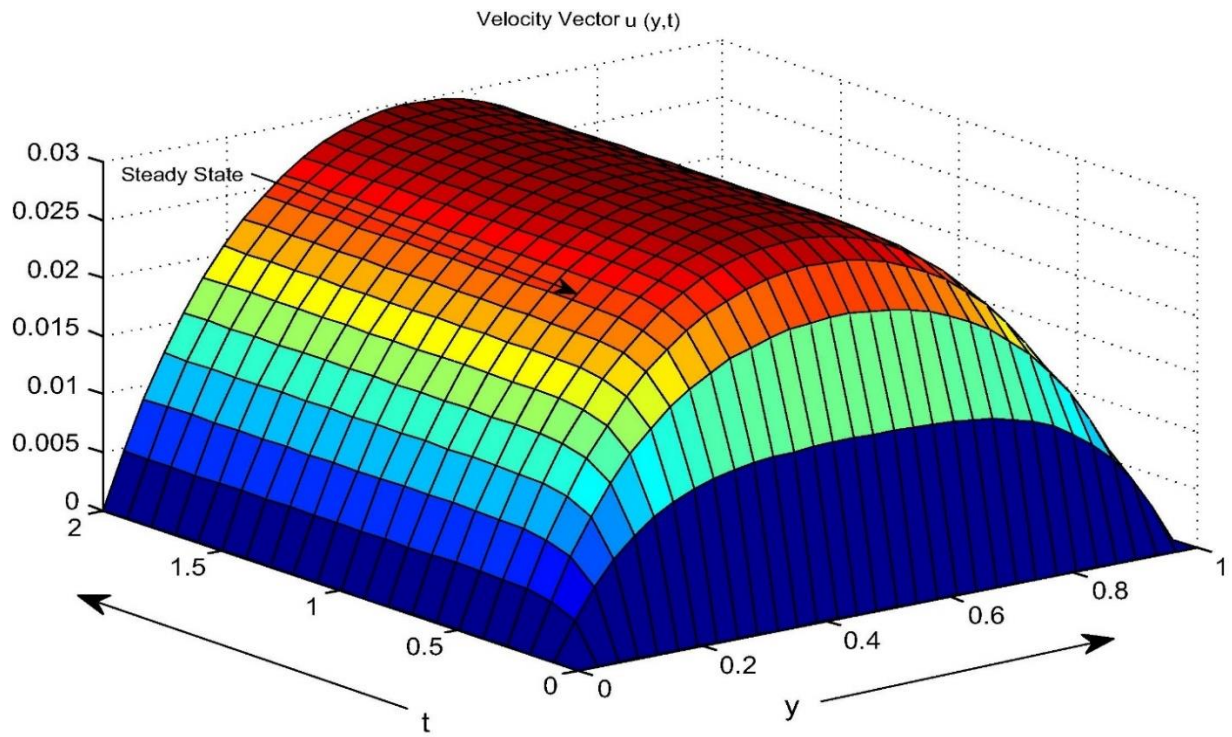


Figure 2.21: Velocity vector $u(y,t)$ for different values of y & t at $m_1 = 1, R = 0.5, b = 0.1, M = 5$ and $Pr = 1$.

In this study, it is focused on the physical parameters M and presented their influences through Figures (2.2) to Figures (2.18) on the velocity, micro-rotation and temperature profiles for asymmetric and symmetric heating of the vertical walls.

Figure 2.2 and Figure 2.3 displays the effect of magnetic parameter M on velocity profiles. It is observed that the amplitude of the velocity as well as the boundary layer thickness decreases when M is increased. The application of a transverse magnetic field results in a resistive type force (called Lorentz force) similar to the drag force, and upon increasing the values of M , the drag force increases which leads to the decelerate of the flow. The influence of material parameter b on velocity profiles is shown in Figure 2.4 & Figure 2.5. In both the thermal cases, It has been observed that velocity of fluid has attained steady state by increase with the time. The graphical results for vortex viscosity R is shown in Figure 2.6 and Figure 2.7. For both thermal cases, it is seen that vortex viscosity parameter has decreased tendency on velocity profiles as well as on steady state time. Figure 2.8 and Figure 2.9 exhibits the velocity profiles for different values of Prandtl number Pr , when the other parameters are fixed. It is highlighted that velocity decreased when Prandtl number Pr is increased. Figure 2.10 and Figure 2.11 are plotted to show the effects of magnetic parameter M on micro-rotation profiles. In both thermal cases, the steady state time and the magnitude of the micro-rotation have increase tendency with the material parameter b . Figure 2.12 and Figure 2.13 displays the effect of material parameter b on the micro-rotation profiles. It is observed that the magnitude of the micro-rotation profile increase with increase in b . The influence of vortex viscosity R on micro-rotation profiles is shown in Figure 2.14 and Figure 2.15. The magnitudes of the micro-rotation profiles increase tendency with R . Figure 2.16 and Figure 2.17 reveal that magnitude of micro rotation decreases with increase in Prandtl number Pr . It is depicted from Figure 2.18 and Figure 2.19 that, the temperature decrease as the Prandtl number Pr increase. It is justified that due to the fact that thermal conductivity of the fluid decrease with increase in Prandtl number Pr and hence decrease the thermal boundary layer thickness. Figure 2.20 and Figure 2.21 display the velocity vectors for different values of t & y at $M = 0.1, b = 0.1, R = 0.5$ and $Pr = 1$ for asymmetric and symmetric cases. From the obtained figures, it reveals that the steady state time in case of asymmetric heating is more than the symmetric heating.

Table 2.1: Numerical and Analytic values of steady state velocity, micro rotation and temperature profile

M	Pr	m_1	R	b	y	Analytic Result for u	Numerical Result for u	Analytic Result for w	Numerical Result for w	Analytic Result for θ	Numerical Result for θ
0.1	1.0	0	0.5	0.1	0.2	0.0320	0.0319	-0.0000783	-0.0000784	0.8000	0.8000
					0.6	0.0373	0.0373	0.0001167	0.0001164	0.4000	0.4000
5	1.0	0	0.5	0.1	0.2	0.0143	0.0144	-0.0000149	-0.0000151	0.8000	0.8000
					0.6	0.0127	0.0127	0.00006198	0.00006189	0.4000	0.4000
0.1	1.0	1	0.5	0.1	0.2	0.0533	0.0533	-0.0002128	-0.0002128	1	1
					0.6	0.0800	0.0800	0.0001064	0.0001064	1	1
5	1.0	1	0.5	0.1	0.2	0.0211	0.0211	-0.0000715	-0.0000717	1	1
					0.6	0.0289	0.0290	0.00003370	0.00003377	1	1
5	0.71	0	0.5	0.1	0.2	0.0143	0.0144	-0.0000149	-0.0000151	0.8000	0.8000
					0.6	0.0127	0.0127	0.00006198	0.00006189	0.4000	0.4000
5	2	0	0.5	0.1	0.2	0.0143	0.0142	-0.0000149	-0.0000151	0.8000	0.7999
					0.6	0.0127	0.0127	0.00006198	0.00006189	0.4000	0.3993
5	0.71	1	0.5	0.1	0.2	0.0211	0.0211	-0.0000715	-0.0000717	1	1
					0.6	0.0289	0.0290	0.00003370	0.00003377	1	1
5	2	1	0.5	0.1	0.2	0.0211	0.0211	-0.0000715	-0.0000717	1	0.9999
					0.6	0.0289	0.0289	0.00003370	0.00003376	1	0.9999
5	1	0	0.5	0.5	0.2	0.0143	0.0144	-0.0000774	-0.0000784	0.8000	0.8000

M	Pr	m_1	R	b	y	Analytic Result for u	Numerical Result for u	Analytic Result for w	Numerical Result for w	Analytic Result for θ	Numerical Result for θ
5	1	0	0.5	1.5	0.6	0.0127	0.0127	0.0003028	0.0003024	0.4000	0.4000
					0.2	0.0144	0.0144	-0.0002489	-0.0002518	0.8000	0.8000
5	1	1	0.5	0.5	0.6	0.0127	0.0127	0.0008599	0.0008589	0.4000	0.4000
					0.2	0.0211	0.0211	-0.0003553	-0.0003562	1	1
5	1	1	0.5	1.5	0.6	0.0289	0.0290	0.0001670	0.0001674	1	1
					0.2	0.0211	0.0212	-0.0010	-0.0011	1	1
5	1	1	0.5	1.5	0.6	0.0290	0.0290	0.0005	0.0005	1	1
					0.2	0.0148	0.0149	-0.0000121	-0.0000122	0.8000	0.8000
5	1	0	0.4	0.1	0.6	0.0129	0.0129	0.00005379	0.00005371	0.4000	0.4000
					0.2	0.0117	0.0131	-0.0000301	-0.0000227	0.8000	0.8000
5	1	0	1.2	0.1	0.6	0.0111	0.0120	0.00009133	0.00007909	0.4000	0.4000
					0.2	0.0217	0.0218	-0.0000607	-0.0000609	1	1
5	1	1	0.4	0.1	0.6	0.0296	0.0296	0.00002851	0.00002857	1	1
					0.2	0.0177	0.0177	-0.0001177	-0.0001179	1	1
5	1	1	1.2	0.1	0.6	0.0177	0.0177	-0.0001177	-0.0001179	1	1
					0.2	0.0249	0.0249	0.0000564	0.0000565	1	1

Table 2.2: Velocity, micro rotation and temperature profile for different step at $M = 0.1, R = 0.5,$
 $b = 0.1, Pr = 1, m_1 = 0$ and $t = 0.5$.

y	u for step size 31 on [0 1]	u for step size 21 on [0 1]	u for step size 11 on [0 1]	w for step size 31 on [0 1]	w for step size 21 on [0 1]	w for step size 11 on [0 1]	θ for step size 31 on [0 1]	θ for step size 21 on [0 1]	θ for step size 11 on [0 1]
0.2	0.0315	0.0315	0.0315	-0.000075	-0.000075	-0.000077	0.7972	0.7972	0.7972
0.4	0.0418	0.0418	0.0418	0.0000114	0.0000110	0.0000091	0.4953	0.5955	0.5954
0.6	0.0365	0.0365	0.0365	0.0001147	0.0001143	0.0001123	0.3955	0.3955	0.3954
0.8	0.0208	0.0208	0.0208	0.0001313	0.0001311	0.0001297	0.1972	0.1972	0.1972

Table 2.3: Velocity, micro rotation and temperature profile for different step size at $M = 0.1,$
 $R = 0.5, b = 0.1, Pr = 1, m_1 = 1$ and $t = 0.5$

y	u for step size 31 on [0 1]	u for step size 21 on [0 1]	u for step size 11 on [0 1]	w for step size 31 on [0 1]	w for step size 21 on [0 1]	w for step size 11 on [0 1]	θ for step size 31 on [0 1]	θ for step size 21 on [0 1]	θ for step size 11 on [0 1]
0.2	0.0523	0.0522	0.0522	-0.000207	-0.000206	-0.000206	0.9944	0.9944	0.9942
0.4	0.0783	0.0782	0.0782	-0.000103	-0.000103	-0.000103	0.9910	0.9907	0.9907
0.6	0.0783	0.0782	0.0782	0.0001032	0.0001032	0.0001032	0.9910	0.9907	0.9907
0.8	0.0523	0.0522	0.0522	0.0002070	0.0002069	0.0002069	0.9944	0.9944	0.9942

Table 2.1 present the comparison of numerical and analytical solution for steady-state velocity, micro rotation and temperature profiles of different values for the magnetic parameter M , vortex viscosity R , material parameter b and prandtl number Pr for asymmetric and symmetric thermal cases. It has seen that, numerical and analytic result are strongly agreement. Table 2.2 and Table 2.3 depict that numerical values of velocity, micro-rotation and temperature profiles are independent of step size for asymmetric and symmetric heating cases.

2.7 Conclusion

An investigation of the effect of magnetic, material and viscosity parameters on free convective flow between two vertical walls in asymmetric and symmetric heating (and cooling) of walls.

The main highlighted points of this study is as follows:

- Prandtl number Pr tends to reduce motion of the fluid and heat transfer process whereas time variable t has reverse effects on it.
- The amplitude of the velocity as well as the boundary layer thickness decrease when magnetic parameter M is increased.
- Magnitude of the micro-rotation has increased tendency with the magnetic parameter M , material parameter b and vortex viscosity R while decrease tendency with Prandtl number Pr .
- The steady state time of fluid velocity as well as micro-rotation is seen more for symmetric cases compared to asymmetric cases.
- The velocity and micro-rotation profiles of fluid decrease at any point of fluid regime with magnetic parameter M .
- The velocity decreases and micro rotation profile increases at any point of fluid regime with vortex viscosity parameter R .
- The steady state time of velocity profile and micro-rotation have decreasing tendency with material parameter b .